Oncogene (2004) 23, 3990–3998

www.nature.com/onc

CpG methylation in the *Fhit* regulatory region: relation to Fhit expression in murine tumors

Shuang-Yin Han[1,6], Dimitrios Iliopoulos[1,6], Teresa Druck[1], Gulnur Guler[1,7], Clinton J Grubbs[2], Michael Pereira[3], Zhongqiu Zhang[4], Ming You[4], Ronald A Lubet[5], Louise YY Fong[1] and Kay Huebner*[,1]

[1]*Kimmel Cancer Center, Thomas Jefferson University, 1008 BLSB, 233S. 10th Street, Philadelphia, PA 19107, USA;* [2]*Department of Surgery, University of Alabama at Birmingham, Birmingham, AL 35294, USA;* [3]*Department of Pathology, Medical College of Ohio, Toledo, OH, USA;* [4]*Department of Surgery, Washington University, St Louis, MO, USA;* [5]*Division of Cancer Prevention and Control, DCPC, National Cancer Institute, Bethesda, MD 20852, USA*

To determine if: (1) 5′ CpG island methylation is related to *Fhit* inactivation; (2) there are tumor or carcinogen-specific methylation patterns, we examined 35 CpG sites in the promoter, exon and intron 1 of the mouse *Fhit* gene. In primary tumors of lung, urinary bladder and tongue, induced by different carcinogens, 15–35% of sites were methylated, with specific methylation patterns associated with each cancer type, suggesting cancer- or tissue-specific methylation patterns. The methylation patterns were associated with reduced Fhit expression, as determined by immunohistochemical analyses. Methylation of rat *Fhit* 5′ CpGs in mammary adenocarcinomas, detected by methylation specific PCR amplification, also correlated with reduced gene expression. Thus, there was an overall association between promoter/exon 1 methylation and decreased Fhit expression. In contrast, in cancer-derived cell lines 70–95% of the CpG sites were methylated. This is the first detailed study of the relationship between *Fhit* 5′ CpG island methylation and Fhit expression in murine tumors, our main models for preclinical cancer studies, and provides evidence that loss of Fhit expression and methylation are correlated in these mouse models and these models will be useful to examine the complex relationships among gene expression, methylation patterns and organ specificity.
Oncogene (2004) **23,** 3990–3998. doi:10.1038/sj.onc.1207526
Published online 8 March 2004

Keywords: CpG island methylation; Fhit promoter; epigenetics; tumor suppressor; gene inactivation; homozygous deletion

Introduction

The human *fragile histidine triad (FHIT)* gene is a tumor suppressor gene for most common forms of cancer, including head and neck, lung, breast, cervical, kidney, gastric and esophageal (Huebner and Croce, 2001). It maps to human chromosome region 3p14.2 and encompasses the chromosomal fragile site, *FRA3B,* a region that appears as a gap or break after exposure to specific replication inhibitors (Ohta *et al*., 1996). The *FHIT* gene is homozygously deleted in numerous cancers and cancer cell lines (Druck *et al*., 1997) and expression of Fhit protein is reduced or lacking in the majority of human cancers, often due to deletions in both alleles (Ohta *et al*., 1996; Sozzi *et al*., 1996; Huebner and Croce, 2001). *Fhit* knockout mice are more susceptible to spontaneous and induced cancers than wild-type mice, with 100% of *Fhit* +/− mice exhibiting forestomach tumors after exposure to *N*-nitrosomethylbenzylamine (NMBA) (Fong *et al*., 2000; Zanesi *et al*., 2001). Tumor development after NMBA treatment can be prevented by oral *FHIT* virus therapy (Dumon *et al*., 2001). The murine *Fhit* locus maps near the centromere proximal *Ptprg* locus on mouse chromosome 14 and the cDNA sequence and structure are similar to those of the human gene, with exons 5–9 encoding the protein (Glover *et al*., 1998; Pekarsky *et al*., 1998). Previous studies have shown that point mutations of *FHIT* are infrequent in cancer cells and structural alterations of the gene have not been detected in many cancers in which the protein is not expressed. Thus, a number of investigators have sought evidence for epigenetic inactivation of the gene in human cancers (Tanaka *et al*., 1998; Zochbauer-Muller *et al*., 2001). There have been many reports concerning methylation of CpGs in control regions of chromosome 3p-linked genes, including *RASSF1A* and *VHL* (Herman *et al*., 1994; Agathanggelou *et al*., 2001).

The 5′ promoter regions of many genes include CpG islands, cytosine–guanosine rich areas. In higher order eukaryotes, DNA may be methylated at cytosines 5′ to guanosines and methylation can affect the level at which a gene is expressed. In 1986, hypermethylation of CpG

*Correspondence: K Huebner; E-mail: K_Huebner@mail.jci.tju.edu
[6]These authors contributed equally to this work
[7]Permanent address: Department of Pathology, Hacettepe University, Ankara, Turkey
Received 22 October 2003; revised 13 January 2004; accepted 16 January 2004; Published online 8 March 2004

islands was reported for the calcitonin gene on chromosome 11p in lung cancer and lymphomas (Baylin *et al*., 1986). Aberrant methylation at CpG islands has been associated with transcriptional repression of tumor suppressor genes such as the *RB* gene in retinoblastoma, *VHL* in renal tumors, *CDKN2A* in bladder cancers and *RARβ, TIMP3, DAPK, RASSF1A* genes in lung and breast cancers, suggesting that it is a mechanism for inactivation of tumor suppressor genes (Gonzalgo *et al*., 1998; Esteller *et al*., 2001). Hypermethylation of 5′ CpG islands of the human *FHIT* gene has been reported in esophageal, lung, breast and bladder cancer, using mainly methylation specific PCR (MSP) (Tanaka *et al*., 1998; Maruyama *et al*., 2001; Zochbauer-Muller *et al*., 2001). One study showed that 5′ CpG island methylation of *FHIT* was detected in 37% of non-small-cell lung cancers (NSCLCs), 31% of primary breast cancers but in 65% of lung and 86% of breast cancer cell lines. Although *FHIT* methylation has typically been associated with decreased Fhit expression, in some Fhit expressing primary NSCLCs and a lung cancer cell line, *FHIT* 5′ CpGs were found to be methylated (Zochbauer-Muller *et al*., 2001).

The DNA methyltransferase (DNMT) inhibitor, 5-Aza-2′-deoxycytidine (5-Aza-CdR), is widely used to study the re-expression of genes silenced by promoter methylation (Cameron *et al*., 1999). In addition, methylated DNA is often associated with deacetylated histones, in accordance with the essential roles of methyltranferases and histone deacetylases (HDACs) in control of expression of endogenous genes. Trichostatin A (TSA), a histone deacetylase inhibitor, participates in reactivation of some repressed genes (Sutherland *et al*., 2001).

Thus far, there are no studies concerning methylation of the *Fhit* alleles of rodents, which serve as the predominant models for carcinogen induction and preclinical prevention and therapy studies. As we have been interested in mechanisms of inactivation of the *FHIT* gene and its role in tumor development, we have investigated in detail the methylation status of the 5′ CpG islands in mouse and rat *Fhit* genes to determine if: (1) Fhit is underexpressed in murine tumors, as in a wide variety of human tumors; (2) methylation of CpG sites is associated with decreased Fhit expression; (3) the methylation state differs in tissues and tumors induced by different carcinogens. We also examined *Fhit* expression and methylation in various mouse cell lines and determined if *Fhit* expression could be reactivated in cell lines by treatment with TSA and 5-Aza-CdR.

Results

Methylation of the Fhit *regulatory region in mouse primary tumors*

We examined 17 mouse primary urinary bladder tumors, five lung tumors and eight squamous cell carcinomas of the tongue by bisulfite genomic sequencing (see Table 2 for primers). The rodent *Fhit* promoter regions were identified by homology to the human *FHIT* promoter region, described in previous reports (Tanaka *et al*., 1998, Zochbauer-Muller *et al*., 2001). In fact, the 5' promoter, exon 1 and flanking intron 1 sequences were very similar in human and mouse. This promoter region retains full activity in reporter gene expression assays (unpublished data). Data for eight bladder tumors (B1–B8), five lung tumors (L1–L5) and six squamous cell carcinomas of the tongue (T1–T6) are summarized in Figure 1. In primary urinary bladder tumors, 23–40% of CpG sites were methylated and, interestingly, three small groups of CpG sites in the promoter (−332 to –227), exon 1 and intron 1 (+168 to +199) were consistently methylated. In addition, nearly the same number (23–35%) of CpG sites were methylated in lung tumors, revealing two regions with a high-frequency of methylation, one between –45 and +32 and the other in intron 1 (+147 to +252), which closely parallels one of the specific methylation areas in bladder tumors. In squamous cell carcinomas of the tongue 14–45% of CpG sites were methylated, with a different distribution of methylated sites (–332 to –227 and +32 to +147), in contrast to the bladder and lung tumors.

Methylation specific PCR amplification

Methylation specific PCR (MSP) amplification was used to examine DNAs from all of the mouse cell lines, primary mouse and rat tumors and normal tissues. The mouse primers anneal specifically either to the methylated or the unmethylated CpG sites at −332, −314 (sense primer) and +32, +40 (antisense primer), while

Table 1 Structure, methylation status and expression of Fhit gene in murine cell lines

Cell lines	*Origin*	*Fhit exons*	*Methylation status*	*Fhit RT–PCR*	
				Before 5-Aza+TSA	*After5-Aza+TSA*
LMTK$^-$	MCA-treated adult connective tissue	+	+	+	+
WEHI164	MCA-induced fibrosarcoma	+	+	+	+
K1735	Melanoma	+	+	–	+
RENCA	Renal carcinoma	−E5	+	NT	NT
MEL	FeLv erythroleukemia	−E6,7,8	+	NT	NT
IT22	3T3 TK$^-$ clone	+	+	–	NT

NT: not tested

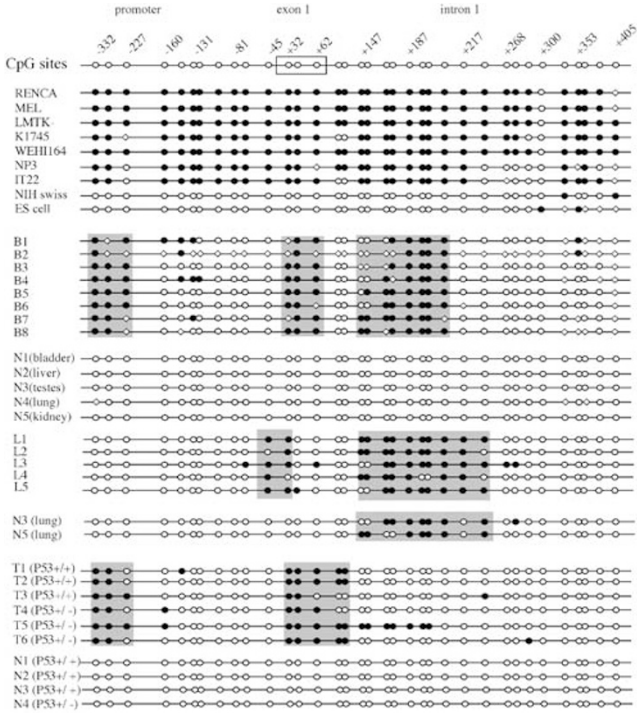

Figure 1 Methylation status of the *Fhit* 5′ CpG islands in murine cell lines, primary tumors and normal tissues. The top line represents the genomic map of CpG sites in the 5′ promoter region of *Fhit*. The numbers above the top line show the positions of the CpG sites analysed relative to the start site of exon 1, which is boxed. The other horizontal lines show the methylation status of individual DNAs as determined by genomic bisulfite sequencing. The first nine DNAs (RENCA through ES cell) are from murine cell lines; B1 through B8 are murine primary bladder tumors; N1 through N5 are normal murine tissues from untreated mice; L1 through L5 are lung primary tumors; N3 and N5 are from nontumor lung tissue from carcinogen treated mice; T1 through T6 are squamous carcinomas of the tongue; N1 through N4 are from nontumor tongue tissue of carcinogen treated mice. Note that N3 and L3 from the same mouse show very similar methylation footprints in intron 1. The diamonds and the filled and empty circles represent hemimethylated, methylated and nonmethylated CpG sites, respectively

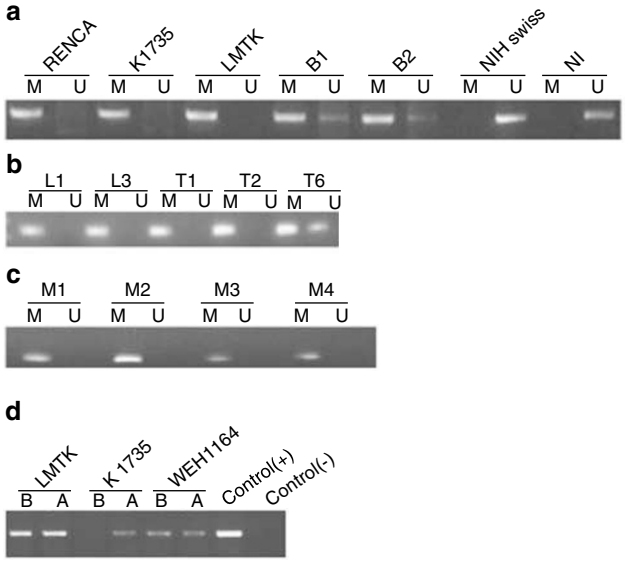

Figure 2 Methylation specific PCR (MSP) amplification of the *Fhit* promoter. Bisulfite-modified DNA was amplified using MSP primers detailed in Table 2. (**a**) Cancer-derived cell lines RENCA, K1735 and LMTK$^-$ clearly show only methylated PCR products; primary bladder tumors B1 and B2 show both methylated and unmethylated PCR products; noncancer-derived cell line NIH swiss kidney and normal bladder tissue N1 show only unmethylated PCR products. (**b**) L1 and L3 primary lung tumors show only the methylated PCR product; T1 and T2 squamous cell carcinomas of the tongue show only the methylated PCR product, while T6 show both methylated and unmethylated PCR products, but the methylated PCR product is stronger. (**c**) M1-4 rat mammary adenocarcinomas clearly show only the methylated PCR product; M: methylated PCR product; U: unmethylated PCR product. (**d**) RT–PCR amplification of *Fhit* transcripts in murine cancer cell lines. Amplified *Fhit* transcripts were observed in LMTK$^-$ and WEHI164, but not in K1735 cells before 5-Aza-CdR treatment. After 5-Aza-CdR treatment *Fhit* was re-expressed in K1735 cells. (**b**) Before 5-Aza-CdR treatment; (**a**) after 5-Aza-CdR treatment

the rat primers anneal specifically either to the methylated or the unmethylated CpG sites at –298, –280 (sense primer) and +191, +193, +198 (antisense primer). MSP clearly showed a methylated amplification product in DNAs from mouse cancer cell lines and IT22 and an unmethylated product in DNA from the normal cell lines and tissues (Figure 2a). We also determined the methylation status of the *Fhit* control regions in tail DNA from *Fhit* +/+, +/−, −/− mice by MSP amplification. These samples showed unmethylated status (data not shown), indicating that the recombinant knockout allele had not become methylated, at least for the four CpGs tested. Both methylation specific and unmethylation specific products were amplified from bladder primary tumor DNAs (Figure 2a). MSP for the lung and tongue tumors revealed mainly the methylation specific product (Figure 2b). MSP amplification from the rat mammary adenocarcinoma DNAs clearly revealed only methylation specific products (Figure 2c).

Fhit expression in primary tissues

The level of Fhit protein or RNA expression was reported for the murine cell lines (Pekarsky *et al*., 1998) and results are included in Table 1. To determine the level of Fhit protein expression in the rat mammary tumors and mouse tongue and bladder tumors, immunohistochemical analysis was performed using anti-mouse Fhit antiserum (Fong *et al*., 2000). This antiserum is specific for Fhit as demonstrated by Western blot using crude lysates from wild-type and *Fhit* knockout mice (Fong *et al*., 2000) and by immunohistochemical analysis of murine tissues. Kidney tissues of wild-type mice were strongly Fhit positive and from Fhit homozygous knockout mice, completely negative (not shown). Fhit protein was reduced or absent in bladder tumors (Figure 3, for examples) and some hyperplasias (Lubet *et al*., 2003) induced by OH-BBN. Fhit immunostaining of the squamous cell carcinomas of the tongue/oral cavity revealed reduced gene expression in all the tumor samples (see Table 3 for summary and Figure 3 for examples). Also, all the rat mammary adenocarcinomas demonstrated significantly decreased or absent expression of Fhit protein (Figure 3).

Table 2 Primers for genomic bisulfite sequencing, methylation specific PCR and RT–PCR

Primer		*Sequence*	*Genomic location*[a]	*Product size(bp)*
Genomic bisulfite sequencing				
PCR	Fhit-F	5′-GGAGATAGGAAGTGAAGTAGTTAGYTT-3′	−363	871
	Fhit-R	5′-ATTCTACAACTRCCCTAAAACCTATTC-3′	+508	
Sequencing	Seq 1R	5′-AAATCCCACAACAAACCCA-3′	−19	
	Seq 2R	5′-CCACTAACTRCCCTAAAACCTATTC-3′	+144	
	Seq 3R	5′-ATTCTACAACTRCCCTAAAACCTATTC-3′	+508	
Methylation specific PCR				
Methylated (mouse)	Fhit-M-F	5′-TTTCGGAGAAAAGTAAAGGAAC-3′	−355	387
	Fhit-M-R	5′-AACGAAAAATACCGCCTAAACG-3′	+52	
Unmethylated (mouse)	Fhit-U-F	5′-TTTTGGAGAAAAGTAAAGGAAT-3′	−335	387
	Fhit-U-R	5′-AACAAAAATACCACCTAAACA-3′	+52	
Methylated (rat)	Fhit-M-F	5′-TTTCGGAGAAAAGTAAGGAAAC-3′	−301	513
	Fhit-M-R	5′-ATTAACCTATCCCCGCCCCGCG-3′	+212	
Unmethylated (rat)	Fhit-U-F	5′-TTTTGGAGAAAAGTAAGGAAAT-3′	−301	513
	Fhit-U-R	5′-ATTAACCTATCCCCACCCCACA-3′	+212	
RT–PCR				
First PCR	Fhit-E2-F	5′-TGAAGCCCAGCAAAGAAG-3′		687
	Fhit-E9-R	5′-AAAGTAGACCCGCAGAGC-3′		
Second PCR	Fhit-E5-F	5′-ACTGTGAGACCATGTCATT-3′		286
	Fhit-E7-R	5′-ACAGTCTGCCCAGCTTCA-3′		

[a]Genomic location of the primers are relative to the start site (+1) of exon 1, our sequence is unpublished, but high throughput genomic sequence for this region is available (AC102468). The underlined bases show the differences between MSP primers Y is C or T, R is A or G

Note that in Table 3, results are given for all the tongue and mammary tumors that were studied for methylation, plus additional tumors for which we had too little DNA for methylation studies. Among the rat mammary tumors, two tumors showed reduced staining in <25% of tumor cells and no staining in >75% (62T1) or moderate staining (75T1) in 26–50% of cells, with the remainder negative. All other mammary adenocarcinomas were >90% negative for Fhit expression. Similarly, as summarized in Table 3, the tongue/oral cavity tumors were all >75% negative for Fhit expression. Three tongue tumors showed moderate-to-strong Fhit expression in fewer than 25% of cells. Noncancerous and dysplastic tongue epithelial cells in the basal cell layer were mostly only weakly positive for Fhit, while the upper squamous layers were more Fhit positive, as shown in Figure 3.

Methylation of the Fhit *gene in cancer cell lines*

We examined the same 35 CpG sites within the promoter, exon 1 and intron 1 of the *Fhit* gene in six mouse cancer-derived cell lines (RENCA, MEL, LMTK$^-$, K1735, WEHI164, NP3), three noncancer-derived mouse cell lines (IT22, NIH Swiss kidney, ES) and five normal tissue samples (bladder, liver, testes, lung and kidney) by bisulfite genomic sequencing, using primers listed in Table 2. We found that DNAs from all mouse cancer cell lines and the IT22 cells exhibited methylation of 71–97% of the CpG sites, in contrast to DNA from five normal tissue DNAs and two normal tissue-derived cell line DNAs that exhibited methylation in, at most, two of 35 sites (Figure 1). Among the cancer-derived cell lines, according to our previous structural analysis of the endogenous *Fhit* alleles (Druck *et al*., 1998; Pekarsky *et al*., 1998), RENCA renal cancer cells show homozygous deletion of *Fhit* exon 5 and MEL erythroleukemia cells homozygous deletion of exons 6 through 8; *Fhit* gene deletions were not detected in the other cancer cell lines (see Table 1 for summary), although the LMTK$^-$ cells, indeed all L cell lines tested, showed homozygous deletion of several exons within the 5′ end of the adjacent *Ptprg* gene (Wary *et al*., 1993).

Re-expression of the Fhit *gene in mouse cancer cell lines*

Methylated DNA is often associated with deacetylated histones, in accordance with the essential roles of both DNMTs and HDACs in silencing expression of endogenous genes. We examined the effect of 5-Aza-CdR (a DNMT inhibitor) and TSA (an HDAC inhibitor) on *Fhit* expression to ascertain whether DNMT and HDAC activities could play a role in the silencing of *Fhit*. *Fhit* RNA was not expressed in K1735, RENCA or MEL cancer cell lines (Table 1). After treatment with 5-Aza-CdR or the combination of 5-Aza-CdR and TSA, we found that *Fhit* mRNA was re-expressed in K1735 cells, although no increase in expression was observed in LMTK$^-$ or WEHI164 (Figure 2d).

Fhit *structure in murine primary tumors*

We have shown that Fhit protein is not expressed in a panel of bladder tumors and hyperplasias (Lubet *et al*., 2003) induced by OH-BBN. Although we observed methylation of the *Fhit* promoter in these tumors, we were interested in examining the *Fhit* loci for deletion, in

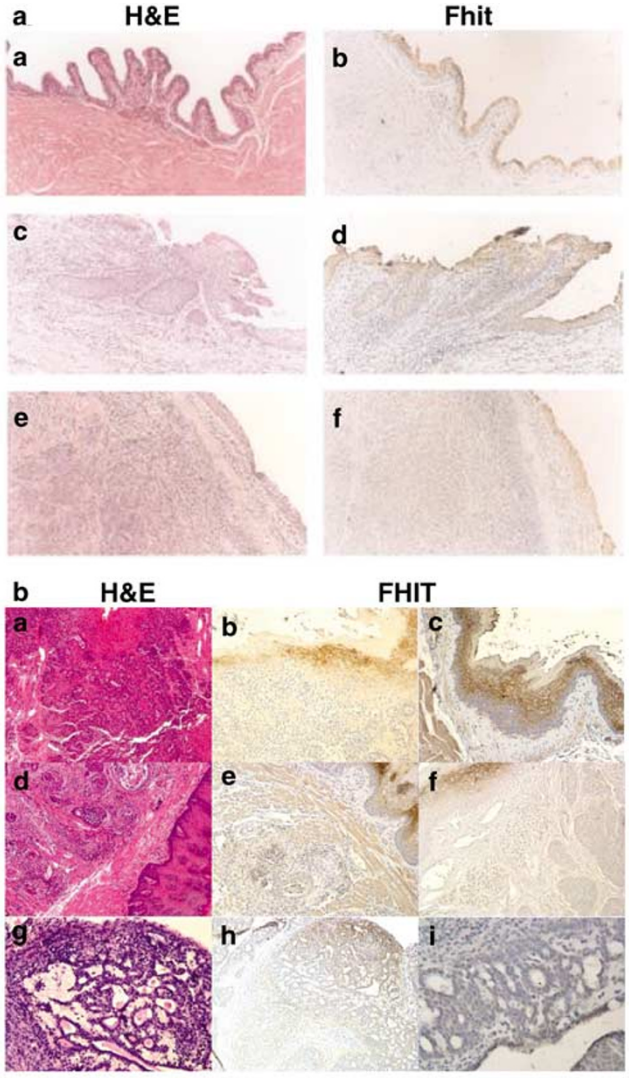

Figure 3 Immunohistochemical detection of Fhit expression. Sections from formalin-fixed tissues of carcinogen-treated mice and rats were placed on slides and one slide per tissue stained with H&E; other slides for each tissue were stained with polyclonal rabbit antiserum specific for rodent Fhit (diluted 1 : 2000). (**a**) Fhit expression in urinary bladder lesions induced by OH-BBN in B6D2F1 mice. Left: Hematoxylin–eosin (H&E) staining. Right: Immunochemistry for Fhit (DAB, cytoplasm stained brown). Normal bladder epithelium shows a single-cell layer (**a**) with strong cytoplasmic staining of Fhit (**b**). Urinary bladder hyperplasia (**c**) shows reduced Fhit staining in lesions but strong staining in epithelial layer (**d**). Urinary carcinoma areas show very reduced or no staining of Fhit (**e**) but moderately strong staining in epithelial layer (**f**) (all $\times$ 100). (**b**) H&E of murine p53+/+12 tongue squamous cell carcinoma (SCC) ($\times$100) (**a**); a section of the same SCC stained with antiFhit ($\times$200) (**b**); a section from the p53+/+12 tumor showing Fhit staining in an esophageal dysplasia ($\times$200) (**c**); H&E of p53+/−9 tongue SCC ($\times$200) (**d**); Fhit staining of a section from p53+/−9 tongue SCC ($\times$200) (**e**); note the staining of the outer squamous epithelium and Fhit expression in muscle; this section of the tongue SCC shows moderate Fhit expression; Fhit staining in p53+/−6 oral cavity SCC which is >90% negative ($\times$200) (**f**); H&E staining of rat mammary adenocarcinoma 64T11 ($\times$200) (**g**); Fhit staining in a nearby section of the same adenocarcinoma ($\times$100) (**h**); Fhit staining of rat mammary adenocarcinoma 74T3 ($\times$400) (**i**)

view of the many cases of inactivation of fragile genes by homozygous deletion. Methylated alleles might be pharmacologically reactivated, if they did not sustain deletions. To examine the *Fhit* gene for structural alterations in primary bladder tumors, *Fhit* exons were probed in five primary bladder tumor DNAs by Southern blot analysis. The results indicated possible deletion within the *Fhit* gene in sample B2 (exon 5) and B6 (exons 5, 9, 10) (Figure 4a). This result suggests that some *Fhit* alleles in primary bladder tumors may have been inactivated by deletions. Possibly some tumors exhibit one deleted *Fhit* allele and one methylated *Fhit* allele.

In addition to Fhit structure analysis based on the restriction enzyme digestion, we used real-time quantitative PCR amplification to examine the relative copy number of exon 5 (the most frequently deleted region of *Fhit* gene) in the primary bladder tumors. The results showed that three of the eight tumor DNA samples examined, tumors B2, B6, and B7, showed reduced copy number of exon 5 alleles relative to the DNA from normal bladder (see Figure 4b). This result is consistent with the Southern blot structural analysis. It is possible that other bladder tumors carry deletions of other *Fhit* exons.

Discussion

Chemically induced tumors in rodents have been used in mechanistic studies, as well as to screen potential chemopreventive and chemotherapeutic agents. Fhit expression is decreased in a wide variety of human tumors, including those of the upper aerodigestive tract, NSCLC, bladder and breast. The major goals in the present study were to characterize murine tumors of various tissues for expression of Fhit and determine the role of methylation in altering Fhit expression in these tumors. As illustrated in Figure 3, Fhit expression was substantially decreased in OH-BBN induced bladder cancers, squamous cell tumors of the upper aerodigestive airways induced by 4NQO and rat mammary adenocarcinomas induced by NMU. Typically, Fhit expression was absent or very weak in the basal layer cells of tongue and oral mucosa, with stronger expression in the upper squamous layers and expression was absent in the resulting tumors. Normal bladder and mammary epithelia express high levels of Fhit, while the bladder and mammary cancers showed little or no expression. In fact, in a parallel study we found that Fhit expression was lost in preinvasive lesions of the bladder, for example, hyperplasias and *in situ* lesions (Lubet *et al*., 2003). We similarly observed minimal expression of Fhit in lung adenomas and adenocarcinomas induced in A/J mice by vinyl carbamate (Dragani and Huebner, unpublished).

Since we observed decreased expression of Fhit in these tumors, we proceeded to examine methylation patterns in the tumors, as contrasted with normal tissue. As can be seen in Figures 1 and 2, we observed methylation of a substantial number of potential CpG

Table 3 Summary of immunohistochemical detection of Fhit in rodent tumors

Oral SCC	*Tissue*	*Diagnosis*	*Fhit status*[a]	*Methylation status*
p53 +/+ T1	Tongue/esophagus	SCC[b]	>90% (−)	Methylated (tongue)[c]
p53 +/+ T2	Tongue/esophagus	SCC	>75% (−), 90% (−)	Methylated (tongue)[c]
p53 +/+ T3	Tongue/esophagus	Ca *in situ*, SCC	>90% (−)	Methylated (tongue)[c]
p53 ± T4	Tongue	SCC	(−)	Methylated[c]
p53 +/+ T5	Tongue/esophagus	SCC	(−)	Methylated (tongue)[c]
p53 ± T6	Tongue	SCC	>75% (−)	Methylated[c]
p53 ± 1a	Tongue	SCC	(−)	
p53 ± 2a	Stomach	SCC	>75% (−)	
p53 +/+ 6	Oral cavity	SCC	>90% (−)	
p53 ± 11	Tongue	SCC	>75% (−)	
Mammary ad.ca				
62 T1	Mammary gland	Adenocacinoma	>75% (−)	Methylated[d]
64 T11	Mammary gland	Adenocacinoma	>90% (−)	Methylated[d]
66 T1	Mammary gland	Adenocacinoma	>90% (−)	Methylated[d]
67 T2	Mammary gland	Adenocacinoma	>90% (−)	Methylated[d]
68 T1	Mammary gland	Adenocacinoma	>90% (−)	Methylated[d]
73 T5	Mammary gland	Adenocacinoma	>90% (−)	Methylated[d]
74 T3	Mammary gland	Adenocacinoma	>90% (−)	Methylated[d]
75 T1	Mammary gland	Adenocacinoma	>50% (−)	Methylated[d]

[a]Proportion of tumor cells that are negative for Fhit. [b]SCC = squamous cell carcinoma; some animals showed both tongue and esophageal cancer and diagnosis is shown for both; if only one diagnosis is shown it refers to both tissues, as does the Fhit staining score. [c]These samples have both MS-PCR and sequencing results. Their detailed methylation status can be seen in Figure 1. [d]These samples have only MS-PCR results, which can be seen in Figure 2c

sites in the promoter region, exon 1 and intron 1 of the *Fhit* gene. Exon 1 is a 5′ untranslated exon. The fraction of potential sites that were methylated was 16–43% and differed significantly between the three different types of mouse tumors. Thus, bladder tumors had the highest % of methylated bases, at ~30%. Methylation was observed in three regions: bases −227 to −332 in the promoter region, +32 to +62 in exon 1 and 160–200 in intron 1. Similarly, the lung tumors showed high degrees of methylation in the intron region, methylation of only one of three sites (base +32) in exon 1, but no methylation in the promoter site (−227 to −332). In the tumors of the oral cavity minimal methylation occurred in the intron region, with methylation in both the promoter and exon 1 region. Thus, each tumor type showed a different, but relatively consistent pattern of methylation, with a common target in exon 1. These results have two important implications. First, each of the tumor types displayed decreased expression of Fhit, as do homologous human tumors (Sozzi *et al*., 1998; Ingvarsson *et al*., 1999; Baffa *et al*., 2000; Skopelitou *et al*., 2001). Secondly, they displayed significant levels of methylation, which may contribute to the decrease in Fhit expression. Since we had observed that certain cell lines, which displayed methylation of the *Fhit* gene, also displayed deletions within the gene, we examined five of the primary bladder tumors for structural alterations within *Fhit* alleles and observed possible deletions in two of the five tumors. Although we cannot determine if deletion or methylation occurred first in these tumors, in the cancer cell lines, for which we have observed both deletion and methylation, it is likely that deletion occurred first because the deletion end points are identical in all cells of a specific cell line and so must have occurred at the time of clonal expansion; methylation, on the other hand, need not have (Clark and Melki, 2002; Soejima *et al*., 2003) occurred identically in all cells, in order to be detected.

One of the most interesting biological findings of these studies is that the methylation patterns for the three types of mouse tumors were relatively consistent for a given type of tumor but differed substantially among tumors from different organs. In fact, the only base that was consistently methylated, albeit not invariably, was in exon 1 at position +32. Based on the other data it would appear that methylation in two of the three regions, promoter, exon 1 or intron 1, is sufficient and is associated with decreased expression of Fhit. There are two possibilities: that the methylation pattern reflects organ specificity or that it is related to the particular carcinogen employed. These data are intriguing since it demonstrates that in all the tumors, Fhit is underexpressed. In some chemically induced animal tumors, the prevalence of genetic aberrations measured by LOH is less frequent than typically observed in human cancers. Among the tumors we examined, the A/J lung system is the most fully studied for genetic changes and shows relatively less LOH than human tumors. These Fhit results suggest the possibility that promoter methylation may be an important mechanism of carcinogenesis. This result is particularly interesting since the demethylating agent, 5-azacytidine, has proven to be a useful chemopreventive agent in the A/J mouse lung cancer model.

In contrast to the strong correlation between methylation and Fhit expression seen with primary tumors, despite the fact that the tumors showed a minority of methylated bases (16–40%), the cell line DNAs showed a different pattern. First, all tumor cell lines exhibited a high frequency of methylated CpGs (67–95%). Secondly, although the cancer cell lines all showed extensive methylation, two of the six (WEHI 164 and LMTK$^-$)

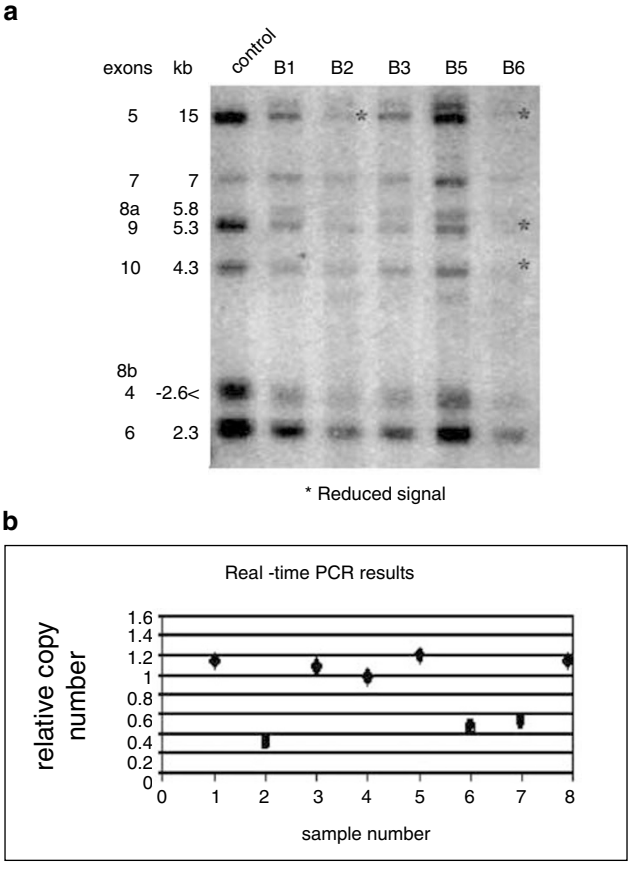

Figure 4 Analysis of the structure of the *Fhit* locus in bladder tumors. (**a**) Southern blot analysis of the *Fhit* locus in primary bladder tumors. *Xba* I-digested genomic DNA was hybridized with a cDNA probe containing exons 4–10 of *Fhit*. The sizes of specific restriction enzyme fragments and the exons contained in these fragments are indicated to the left of the blot. The comparison of hybridization intensities was carried out using ImageQuant 5.1 software and suggested that primary tumor B2 has some loss of exon 5 and tumor B6 a reduction of signal for exons 5, 9, and 10. Lane 1, K1735 DNA (control); Lanes B1–B6, primary bladder tumor DNAs B1, B2, B3, B5, and B6, respectively. Note that K1735 cells are from a B6 inbred mouse while the bladder tumors are from B6D2F1 mice and thus exhibit polymorphisms for some *Fhit* exons. (**b**) Scatter plot of real-time quantitative PCR results. Copy number ratios for samples B2, B6, B7 (not in Southern blot) are within the confidence interval for heterozygous deletion (0.36–0.58); confidence interval for normal copy number is 0.85–1.2. • and ◆ represent sample with deletion and normal copy number respectively

showed expression of *Fhit* mRNA, although the levels were lower than observed in cell lines with unmethylated *Fhit* alleles. Compared with the cancer-derived cell lines, the methylated CpG sites in primary tumors were fewer, consistently with a recent study showing higher levels of CpG island hypermethylation in cancer cell lines than primary tumors (Paz *et al*., 2003). Another feature of *Fhit* promoter methylation in primary tumors was evidence of hemi-methylation at some cytosines; that is, one allele methylated and one not, as indicated by C/T sequence at some residues in the sequence. Other possible explanations for C/T residues are contamination of tumor samples with normal tissue or heterogeneity within the tumor population.

Interestingly, specific groups of CpG sites were consistently methylated in the primary tumors and different types of tumors exhibited different methylation patterns. The methylation pattern of the 5′ CpG island of the *Fhit* gene in most of the samples was very similar to the pattern described by Tanaka *et al*. (1998), and indicated that the region between nucleotides 195 and 283 is sensitive to methylation. Possibly these specific CpG sites are important in gene silencing, suggesting that the hypermethylation observed in DNA from cell lines might have occurred during culture. Mouse lung tumor DNAs were highly methylated in intron 1, as were bladder tumor DNAs, but interestingly, DNA from two normal lung tissues, derived from the mice with lung tumors, were methylated in the same region, suggesting that *Fhit* methylation in these DNAs could be a result of exposure to the carcinogen, vinyl-carbamate.

Perhaps the most important aspect of these studies is that it suggests use of mouse tumors of various organs for studying the role of *Fhit* in prevention or therapy. Modulation by chemopreventive agents of methylation of *Fhit* and other tumor suppressor genes might be useful as a surrogate end point biomarker in clinical trials. We have identified four different types of carcinogen-induced tumors in which *Fhit* inactivation occurs, possibly primarily via methylation, thus allowing testing of genetic and pharmacologic approaches to enhancing Fhit expression as a preventive or therapeutic mechanism. In fact, we have previously shown that the demethylating agent 5-Aza-CdR shows significant efficacy as a chemopreventive agent for A/J mouse lung tumors. We can now determine if it specifically alters methylation of *Fhit* and other tumor suppressor genes.

Materials and methods

Cell lines, tumor and normal tissues

Six murine cancer-derived cell lines, RENCA (renal cancer), MEL (erythroleukemia), LMTK$^-$ (fibrosarcoma), K1735 (melanoma), WEHI164 (fibrosarcoma) and NP3 (myeloma), as well as three noncancer-derived cell lines, NIH Swiss kidney, an ES cell line and IT22 (a late passage, thymidine kinase deficient clone derived from a murine 3T3 line), were grown in MEM (Gibco, Rockville, MD, USA) with 10% fetal bovine serum and 0.1 mg/ml gentamycin (see Table 2 for summary of characteristics of cell lines) (Pekarsky *et al*., 1998). In total, 17 murine urinary bladder cancers (B1-17) were collected from male B6D2F1 mice that received the carcinogen hydroxybutyl(butyl)nitrosamine (OH-BBN) (Grubbs *et al*., 2000). Five normal tissue samples (N1-urinary bladder, N2-liver, N3-testes, N4-lung and N5-kidney) from untreated B6D2F1 mice and three tail tissue samples from *Fhit* +/+, +/− and −/− mice were included in the analyses. DNA was also prepared from mouse lung tumors (L1-5) from mice that received the carcinogen vinyl carbamate, two nontumor lung samples from the treated L3 and L5 mice, eight tongue tumors (T1-8) and four nontumor samples from UL53-3 mice with different genetic backgrounds (p53 wt or p53+/−) that received the carcinogen 4-nitroquinoline-1-oxide (4NQO). In addition, we examined 8 methylnitrosourea (MNU) induced mammary adenocarcinomas (M1-8) that were induced in female Sprague–Dawley rats.

Bisulfite modification

DNA was prepared from cell lines and tissue samples by standard methods and bisulfite modification was performed as reported (Herman *et al*., 1996). Briefly, 3 μg of genomic DNA was denatured in 0.3 M NaOH at 37°C for 15 min and treated with 0.5 mM hydroquinone (Sigma, St Louis, MO, USA) and 2.6 M sodium bisulfite, pH 5 (Sigma, St Louis, MO, USA) at 50°C for 19 h. Modified DNA was purified using Wizard DNA purification resin (Promega Corp., Madison, WI, USA), denatured as above in NaOH, ethanol precipitated and resuspended in 20 μl water. Modified DNA was stored at −20°C until use.

Bisulfite genomic sequencing

Bisulfite-modified genomic DNA (2 μl) was used for PCR amplification. PCR conditions were as follows: 94°C for 5 min, followed by 30 cycles of 94°C for 30 s, 58°C for 30 s, 72°C for 60 s and finally 72°C for 5 min. The PCR product was analysed on 1% agarose gel and purified with Qiagen gel extraction kit (Qiagen, CA, USA). Genomic sequencing of bisulfite-modified DNA was accomplished using the BigDye terminator reaction chemistry for sequence analysis on the ABI Prism 377 (Applied Biosystems, Foster City, CA, USA). Primers used for amplification and sequencing reactions are listed in Table 1.

Methylation specific PCR (MSP)

Specific primers covering CpG sites were designed to distinguish between methylated and unmethylated sequences of bisulfite-modified DNA (Table 2). The PCR mixture contained 1 × PCR buffer, 1.25 mM dNTPs, 10 pmol of each primer, 50 ng bisulfite-modified DNA in a final volume of 25 μl. Reactions were hot-started at 95°C for 5 min before adding 1 U *Taq* polymerase, followed by 30 cycles of 94°C for 30 s, 60°C for 30 s, 72°C for 30 s and a final extension at 72°C for 5 min. PCR products were analysed on 1–2% agarose gels.

5-Aza-2′-deoxycytidine and TSA treatment

Cells were plated at a density of 5×10^5 cells/100 mm dish and treated after 24 h with 5 μM 5-Aza-CdR (Sigma, St Louis, MO, USA) for 5 days or with 1 μM TSA (Sigma, St Louis, MO, USA) for 2 days. Reagent and medium were exchanged every day. To assess the effect of a combination of 5-Aza-CdR and TSA, cells were exposed sequentially to 5-Aza-CdR for 2 days and then to TSA for an additional 2 days.

RNA preparation and RT–PCR

Total RNA from the cell lines was isolated using the RNeasy Mini kit (Qiagen, CA, USA). In total, 2 μg of DNase I-treated total RNA was used for cDNA synthesis. Reverse transcription reaction was performed in 30 μl volume of 1 × first-strand buffer, 10 mM DTT, 3.75 mM of each dNTP, 100 pmol of oligo dT primer, 200 U of MuLV reverse transcriptase (Life Technologies Inc., Rockville, MD, USA). The samples were incubated at 37°C for 90 min, followed by boiling for 5 min. In all, 1 μl of the reaction was used for PCR amplification. PCR primers are shown in Table 2. The PCR consisted of an initial denaturation step at 95°C for 3 min, followed by 25 cycles of 94°C for 30 s, 60°C for 30 s, 72°C for 60 s. A measure of 1 μl from a 1 : 20 dilution of the first round product was used for a second round PCR amplification reaction under the same conditions. PCR products were visualized by ethidium bromide staining of a 2% agarose gel.

Southern blot analysis

To determine if the *Fhit* gene was intact in primary tumors, Southern blot analysis was carried out. DNA from frozen primary tumor tissue was extracted by standard methods. Genomic DNA (5 μg) was digested with *Xba* I restriction enzyme and blotted to nylon membrane (Hybond N^+, Amersham). cDNA from exon 4 through 10 of the *Fhit* gene was labeled with [^{32}P]dCTP and hybridized to the *Xba* I digested tumor DNA. The signal was visualized by Variable Mode imager (Typhoon 8600, Amersham Pharmacia Biotech) and hybridization intensities were analysed with ImageQuant 5.1 software.

Immunohistochemistry

Mouse sections were deparaffinized, rehydrated in a graded alcohol series and heated in 0.01 M sodium citrate (pH 6.0) in a microwave (90°C), for three 5-min periods). Nonspecific binding sites were blocked with 10% goat serum (room temperature for 1 h) and sections were incubated with rabbit anti-mouse Fhit antiserum (Fong *et al*., 2000) at a 1 : 2000 dilution (overnight, in a humidified box), then with biotinylated goat anti-rabbit antiserum (1 : 750 dilution) and finally with streptavidin horseradish peroxidase (1 : 1000 dilution). The location of Fhit protein was visualized by incubation with 3,3-diaminobenzidine tetrahydrochloride (Sigma-Aldrich, St Louis, MO, USA) and the sections were lightly counterstained with hematoxylin. Cells with a brown reaction product in the cytoplasm were defined as positive for Fhit. Tumors were scored as negative (−), weakly or moderately positive, with the outer squamous epithelium of oral cavity/tongue and normal mammary gland tissues representing strong positives. Some tumors expressed Fhit heterogeneously, with the total staining score representing the expression level observed in >75% of the tumor cells. Specificity of mouse Fhit antiserum was described in Fong *et al*. (2000). Briefly, Western blots from cells with homozygous deletions within the Fhit coding region were completely negative for the 16.8 kDa Fhit protein and sections of kidney tissue from Fhit knockout mice tested by immunohistochemical analysis were negative while wild-type kidney sections were strongly positive and Fhit +/− tissues were intermediate.

Real-time quantitative PCR Amplification

Real-time quantitative PCR amplifications were performed to detect genomic deletions based on fluorescent SYBR Green I dye methodology (Nigro *et al*., 2001; Kolomietz *et al*., 2003). Briefly, primers flanking *Fhit* exon 5 were designed to examine this frequently deleted region of *Fhit*, forward primer 5′-TCATCAAGCCCTCTGTGGTTT-3′, reverse primer 5′-AGGCTGGTTCAGTGCTAATTT-3′. The *β-actin* and GAPDH genes were chosen to serve as reference controls for copy number determinations (*β-actin* forward primer, 5′-TGTTACCAACTGGGACGACA-3′, reverse primer 5′-CTGGGTCATCTTTTCACGGT-3′; GAPDH forward primer 5′-AACCACGAGAAATATGACAACT-3′, reverse primer 5′-CAAAGTTGACATGGATGACCTT-3′). Each sample and control (one normal calibrator control and one no-template control) was run in triplicate for both target and reference sequences. Reactions (25 μl) consisted of: 12.5 μl 2 × SYBR green Master mix (Applied Biosystem, UK), 400 nM forward primer, 400 nM reverse primer and 20 ng of template DNA. The thermal cycling conditions were 95°C for 10 min, followed by 40 cycles of 95°C for 15 s and 60°C for 1 min. The number of cycles required for reporter dye fluorescence to

exceed background level was defined as the cycle threshold (Ct) and was automatically estimated using ABI PRISM 7700 Sequencing Detection System (PE Applied Biosystems, Foster city, CA, USA). The starting relative copy number of the *Fhit* gene in tumor DNA samples was determined using a comparative $2^{-\Delta\Delta Ct}$, in which $\Delta\Delta Ct = \Delta Ct^{tumor} - \Delta Ct^{normal}$ and each $\Delta Ct = Ct^{target} - Ct^{ref}$.

Acknowledgements
This research was supported by National Cancer Institute Contract N01-CN-15128, N01-CN-15113, N01-CN-25007, a subaward from Ohio Medical College, as well as grants CA77738 and CA56036 from the National Cancer Institute. Gulnur Guler was supported by funding from the University of Hacettepe and from the National Institutes of Health.

References

Agathanggelou A, Honorio S, Macartney DP, Martinez A, Dallol A, Rader J, Fullwood P, Chauhan A, Waler R, Shaw JA, Hosoe S, Lerman MI, Minna JD, Maher ER and Latif F. (2001). *Oncogene*, **20,** 1509–1518.

Baffa R, Gomella LG, Vecchione A, Bassi P, Sedor J, Calviello CM, Gardiman M, Minimo C, Strup SE, McCue PA, Kovatich A, Pagano F, Huebner K and Croce CM. (2000). *Am. J. Pathol.*, **156,** 419–424.

Baylin SB, Hoppener JW, de Bustros A, Steenbergh PH, Lips CJ and Nelkin BD. (1986). *Cancer Res.*, **46,** 2917–2922.

Cameron EE, Bachman KE, Myohanen S, Herman JG and Baylin SB. (1999). *Nat. Genet.*, **21,** 103–107.

Clark SJ and Melki J. (2002). *Oncogene*, **21,** 5380–5387.

Druck T, Berk L and Huebner K. (1998). *Oncol. Res.*, **10,** 341–345.

Druck T, Hadaczek P, Fu TB, Ohta M, Siprashvilli Z, Baffa R, Negrini M, Kastury K, Veronese ML, Rosen D, Rothstein J, McCue P, Cotticelli MG, Inoue H, Croce CM and Huebner K. (1997). *Cancer Res.*, **57,** 504–512.

Dumon KR, Ishii H, Fong LY, Zanesi N, Fidanza V, Mancini R, Vecchione A, Baffa R, Trapasso F, During MJ, Huebner K and Croce CM. (2001). *Proc. Natl. Acad. Sci. USA*, **98,** 3346–3351.

Esteller M, Corn PG, Baylin SB and Herman JG. (2001). *Cancer Res.*, **61,** 3225–3229.

Fong LYY, Fidanza V, Zanesi N, Lock L, Siracusa L, Mancini R, Siprashvili Z, Ottery M, Martin SE, Druck T, McCue PA, Croce CM and Huebner K. (2000). *Proc. Natl. Acad. Sci. USA*, **97,** 4742–4747.

Glover TW, Hoge A, Miller DE, Ascara-Wilke JE, Adam A, Dagenais SL, Wilke CM, Dierick HA and Beer DG. (1998). *Cancer Res.*, **58,** 3409–3414.

Gonzalgo ML, Hayashida T, Bender CM, Pao MM, Tsai YC, Gonzales FA, Nguyen HD, Nguyen TT and Jones PA. (1998). *Cancer Res.*, **58,** 1245–1252.

Grubbs CJ, Lubet RA, Koki AT, Leahy KM, Masferrer JL, Steele VE, Kelloff GJ, Hill DL and Seibert K. (2000). *Cancer Res.*, **60,** 5999–6002.

Herman JG, Graff JR, Myohanen S, Nelkin BD and Baylin SB. (1996). *Proc. Natl. Acad. Sci. USA*, **93,** 9821–9826.

Herman JG, Latif F, Weng Y, Lerman MI, Zbar B, Liu S, Samid D, Duan DSR, Gnarra JR, Linehan WM and Baylin SB. (1994). *Proc. Natl. Acad. Sci. USA*, **91,** 9700–9704.

Huebner K and Croce CM. (2001). *Nat. Rev. Cancer*, **1,** 214–221.

Ingvarsson S, Agnarsson BA, Sigbjornsdottir BI, Kallioniemi OP, Barkardottir RB, Kovatich A, Schwarting R, Hauck WW, Huebner K and McCue PA. (1999). *Cancer Res.*, **59,** 2682–2689.

Kolomietz E, Marrano P, Yee K, Thai B, Braude I, Kolomietz A, Chun K, Minkin S, Kamel-Reid S, Minden M and Squire JA. (2003). *Leukemia*, **17,** 1313–1323.

Lubet RA, Fong LY, Huebner K, Altieri DC, Steele VE, Kopelovich L, Kavanaugh C, Juliana MM and Grubbs CJ. (2003). *Carcinogenesis* (submitted).

Maruyama R, Toyooka S, Toyooka KO, Harada K, Virmani AK, Zochbauer-Muller S, Farinas AJ, Vakar-Lopez F, Minna JD, Sagalowsky A, Czerniak B and Gazdar AF. (2001). *Cancer Res.*, **61,** 8659–8663.

Nigro JM, Takahashi MA, Ginzinger DG, Law M, Passe S, Jenkins RB and Aldape K. (2001). *Am. J. Pathol.*, **158,** 1253–1262.

Ohta M, Inoue H, Cotticelli MG, Kastury K, Baffa R, Palazzo J, Siprashvili Z, Mori M, McCue P, Druck T, Croce CM and Huebner K. (1996). *Cell*, **84,** 587–597.

Paz MF, Fraga MF, Avila S, Guo M, Pollan M, Herman JG and Esteller M. (2003). *Cancer Res.*, **63,** 1114–1121.

Pekarsky Y, Druck T, Cotticelli MG, Ohta M, Shou J, Mendrola J, Montgomery JC, Buchberg AM, Siracusa LD, Manenti G, Fong LY, Dragani TA, Croce CM and Huebner K. (1998). *Cancer Res.*, **58,** 3401–3408.

Skopelitou AS, Gloustianou G, Bai M and Huebner K. (2001). *In vivo*, **15,** 169–173.

Soejima K, Fang W and Rollins BJ. (2003). *Oncogene*, **22,** 4723–4733.

Sozzi G, Veronese ML, Negrini M, Baffa R, Cotticelli MG, Inoue H, Tornielli S, Pilotti S, De Gregorio L, Pastorino U, Pierotti MA, Ohta M, Huebner K and Croce CM. (1996). *Cell*, **85,** 17–26.

Sozzi G, Pastorino U, Moiraghi L, Tagliabue E, Pezzella F, Ghirelli C, Tornielli S, Sard L, Huebner K, Pierotti MA, Croce CM and Pilotti S. (1998). *Cancer Res.*, **58,** 5032–5037.

Sutherland JE, Peng W, Zhang Q and Costa M. (2001). *Mutat Res.*, **479,** 225–233.

Tanaka H, Shimada Y, Harada H, Shinoda M, Hatooka S, Imamura M and Ishizaki K. (1998). *Cancer Res.*, **58,** 3429–3434.

Wary K, Lou Z, Buchberg A, Siracusa L, Druck T, LaForgia S and Huebner K. (1993). *Cancer Res.*, **53,** 1498–1502.

Zanesi N, Fidanza V, Fong LY, Mancini R, Druck T, Valtieri M, Rudiger T, McCue PA, Croce CM and Huebner K. (2001). *Proc. Natl. Acad. Sci. USA*, **98,** 10250–10255.

Zochbauer-Muller S, Fong KM, Maitra A, lam S, Goradts J, Ashfuq R, Virmani Ak, Milchgrub S, Gazdar AF and Minna JD. (2001). *Cancer Res.*, **61,** 3581–3585.